

Torsional Loading Behaviors of Slotted Filament Wound Glass Fiber Reinforced Composite Tubes

*İbrahim Fadıl Soykök(0000-0001-8392-4505)

*Department of Mechatronics Engineering, H.F.T. Faculty of Technology,
Manisa Celal Bayar University, 45400 Turgutlu, Manisa, Turkey
ifsoykok@gmail.com

Received Date: 01.02.2018

Accepted Date: 02.04.2018

Abstract

The stress and strain behaviors of filament wound glass-fiber epoxy based cylindrical tube structures made of two different stacking sequences as $[(\pm 45^\circ)_5]$ and $[(0/90)_5]$ were numerically investigated under a constant torque value. The exterior surfaces of tubes were deliberately defected by longitudinally extending, rounded end, 0.6 mm deep, 2 mm wide but varying-length slots. Slot-less and full-length-slot structures were also included in the study. During torsional loading, the variations in stresses, strains and twisting angles of the specified thin-walled composite tube models were investigated, comparatively. Additionally, the effects of fiber winding angles and slot lengths on the specified quantities were parametrically examined. A considerable amount of stress accumulation around the slot tip of both type of tube model is measured which constitute a risk of damage progression. At the innermost laminas, slight fluctuations in the maximum stresses are observed in the slot lengths shorter than 140mm, whereas rapid increases are remarkable for exceeded lengths. On the other hand, the maximum stress changes in the outermost layer are quite uneven. From slot-less to full-length-slot, the change in slot dimensions provokes 8.32 and 9.11 % increments in twisting angles in the $45^\circ/-45^\circ$ angle-ply and $0^\circ/90^\circ$ cross-ply structures, respectively. Under the same loading condition, $[(\pm 45^\circ)_5]$ stacking sequence gives the structure averagely 0.66° lower total rotation at the specimen tip in comparison to $[(0/90)_5]$ fiber arrangement.

Keywords: Filament winding, Glass-fiber epoxy, Composite tubes, Torsion

1. INTRODUCTION

Due to the rapidly expanding use of composite materials especially in aerospace, automotive and marine industries, investigating the multi-axial tensile stresses both numerically and experimentally has become more important since a few decades. Hollow cylindrical components, which are generally designed as carrier bars in vehicle bodies, can meet different challenges, such as bending, torsion and buckling, simultaneously or alternatively. This study will generally be based on a numerical examination of the effect of the torsional moments on the glass-fiber / epoxy tubes produced by filament winding technique. Because of the anisotropic nature of the material, numerous experimental studies have been conducted so far and they have been verified and supported by numerical examinations like the current one.

In a study by Meijer and Ellyin [1], multi-axial experimental tests of tubes produced by filament winding method showed that the first faults and fracture occur in the outer shell. The

specimens tested for various axial stresses to the internal stress ratios was adjusted to the MTS test system prior to applying axial force and internal pressure simultaneously. Five different failure modes such as spiral cracks, regional leakages and axial collapses were observed on the tubes exposed to aforesaid load ratios. Burda et al. [2] studied sintered glass fiber polymer matrix composite bars produced industrially for various applications. Beside these bars, a double console beam specimen is also designed for delamination tests in semi-static mode. During the investigation of the case, the size and shape of the test specimens, the load starting type, and different pre-cracking methods were examined.

Perillo et al. [3] reported a complete application procedure which was used to evaluate the performance of the newly developed test methodologies for composite filament wound composites produced from glass-vinilester and carbon-epoxy materials which are known as essential for making some aircraft components. In the new method developed for biaxial testing, an arrangement is made to reduce the stress

*Corresponding author: Department of Mechatronics Engineering, H.F.T. Faculty of Technology,
Manisa Celal Bayar University, 45400 Turgutlu, Manisa, Turkey, ifsoykok@gmail.com, GSM: +905367904411

concentration at the sample edges. Furthermore, the amount of void space produced by the newly applied optical method has been evaluated.

Martins et al.[4] applied internal pressure to filament wound composite tubes in order to find out burst pressures. Closed-end four thin-walled and various wind angle E-glass fiber/epoxy tube models were subjected to pressure loading by employing an alternative damage method. In terms of the leakage and burst failure pressures numerical results performed in ABAQUS and experimental data showed a good agreement. As a follow up study Martins et al.[5] performed progressive failure analysis by using finite element method in order to determine the minimum specimen length for representing infinite tube, to find the optimum wind angle and the influence of diameter and thickness on the tubes subjected to internal pressure. The parametric study has given optimum wind angles of 53.25, 74.5 and 88 degrees for closed, restrained and open-end conditions, respectively. It was also found that the failure pressure changes linearly in accordance with h/R (mean thickness / Radius) ratio.

Morozov [6] draws the attention on some manufacturing effects of filament winding process. The study claims that the filament-winding mosaic pattern of the composite layer has not been taken into account in previous studies which could significantly affect the stress and strain fields in the thin-walled composite structure. Actually, this effect has been clearly demonstrated numerically by using particular examples.

Hafeez and Almaskari by V shaped cradles at each end. The compliance of behavior with the scaling law of Buckingham Pi theorem was investigated with tests for four different scales. Contrary to the previous findings, semi-circular cradle supported specimens resting on V support have given[7] applied lateral indentation to glass fiber / epoxy filament wound thin walled tubes supported higher loads and bigger damage area for same indentation displacement. The load required for delamination initiation has been found same for both floor supported and V supported specimens.

Xing et al. [8] analyzed varying winding angle structures under axial loading, internal and external pressure. First the results related to deformation and stresses of orthotropic layers were obtained, analytically and then they were compared with the numerical data. The usage of multi angle filament-wound composites has been found to increase material utilization and working pressure. Interestingly, it was found that a constant through thickness strength for multi angle wound cylindrical vessel under internal pressure is obtained by applying gradual bigger winding angle outward. Another study conducted by Mertiny et al. [9] maintains also considerable advantages of multi-angle winding technology over pure angle-ply lay-ups. The performances of multi-angle and $\pm \alpha$ angle-ply lay-up filament wound structures were compared by assessing experimental results in terms of failure stresses, failure

modes and stress-strain curves. Under various loading conditions, multi-angle wound structures exhibited an overall better performance in resisting damage.

Krishnan et al. [10] performed a multi-axial cycling loading on glass/epoxy composite tubes with different winding angles. By the aid of a novel test equipment, the tubes with three different winding angles were subjected to five stress ratios from pure axial to pure hoop loading. The results showed a strong relation between optimum winding angle and the ratio of applied stresses.

Loading condition is a deterministic factor affecting mechanical response of filament wound composite tubes having diverse winding patterns. As an alternative loading type, Moreno et al. [11] studied external pressure behaviors of cylindrical specimens having stacked layers with coincident patterns in a hyperbaric testing chamber. Buckling pressures and modes of thin walled cylinders were predicted analytically and verified by experimental results. Buckling behavior of cylinders did not seem to be influenced by two chosen winding patterns, whereas, length to diameter ratio and thickness have very expectedly a direct influence on the buckling response.

As can be seen in the previous studies, the winding pattern and loading conditions is regarded as the main factors influencing under load behavior and failure response of filament wound composite tubes in design. However if the tube has been damaged somehow, its ability to carry on functioning until replaced or repaired becomes more important. Deep scratches created by a pointed tip are one of the most significant damages which result in stress concentrations triggering a sudden breakage or deformation of the thin walled cylindrical structure. In the present study, the specified scratch damage was tried to be modeled with a rectangular-cross-section wedge slot formed longitudinally on the outer wall of the tubes. The results of two different types of winding e.g. cross-ply (0° - 90°) and angle-ply (45° / -45°) is identified parametrically, while examining the effects of different lengths of slots on stress distribution and angle of distortion.

2. MODEL GEOMETRY, MATERIAL AND LOADING CONDITIONS

Consider a thin walled hollow cylindrical tube with the outer and inner diameters of 18 mm and 16 mm, respectively. Through 1 mm thickness in radial direction, the tube has ten orthotropic layers each of which has 0.1 mm thickness. The fiber orientations of each adjacent plies of the tube are different which gives the structure resistance under multi-axial loading. Fiber orientation angle, the angle between fibers and rotation axis is formed as $\pm \theta$ at each sub-laminate due to the nature of the filament winding process. This angle is automatically adjusted by filament winding device (Fig. 1) by means of controlling the rotation speed of the mandrel and the linear motion rate of the horizontal carrier [12].

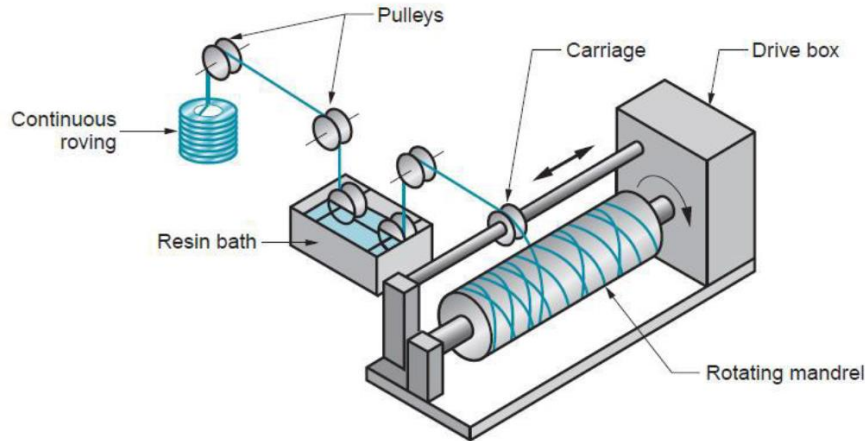


Fig.1 : Schematic illustration of filament winding process (Tele *et. al*,2016)

All of the specimens discussed within the scope of this paper is exposed to a fixed torque of 10 Nm in order to evaluate the actual influence of geometrical defects on the maximum stresses, strains and twist angles. The specimens are of 180 mm length which is an adequate length to extract accurate values of twist angles for each structure geometry. Although D5448/D5448M [13] Standard Test Method for In-plane Shear Properties of Hoop Wound Polymer Matrix Composite Cylinders gives useful definition of clamping fixture to apply torsional moment, the tube's geometrical values is not restricted and not defined for the current specific procedure. Nevertheless, the size and dimensions of the sample has been chosen from among the most encountered in practice. Two different types of stacking sequence that constitute the thin-walled epoxy based glass-fiber reinforced tube structure have been studied. One of them is selected as an angle-ply laminate structure having 10 equal-thickness layers of $[(\pm 45^\circ)_5]$ fiber orientations [14]. The latter is a $[(0/90)_5]$ fiber orientated cross-ply laminate structure manufactured by coating the pre-preg sheets around the mandrel. It is also made of 10 equal-thickness laminas. Because filament wound process allows to be produced merely angle-ply laminas, making use of the

pre-preg layers is essential for creating a cylindrical structure with fibers oriented at 0 and 90 degrees.

In order to model the effects of deep scratches that may have been created by any sharp point during operation and is considered to weaken the structure, 2 mm wide, 0.6 mm deep rectangular cross-section wedge slots were processed on the outer surfaces of the filament wound tubes in the longitudinal direction. This means that a total of six layers inward from the outer surface to the radial direction are affected by the grooving process. Providing that the slot depths and widths stay fixed, the effect of variations in slot lengths on torsional behavior of the tubes made of two alternate layered compositions was investigated parametrically. As listed in Table 1, 18 different types of specimen were defined according to their slot dimensions and corresponding locations. In order to illustrate the slot positioning on the tube geometry, Fig. 2 is given as an example representing the type 6 slotted specimen. It is worth noting that, the type 1 specimen stands for the slot-less model for the purpose of defining a perfect and non-damaged specimen. The torsional responses of the two different material designs of non-slot specimens ($0^\circ / 90^\circ$ and $45^\circ / -45^\circ$) were also examined separately.

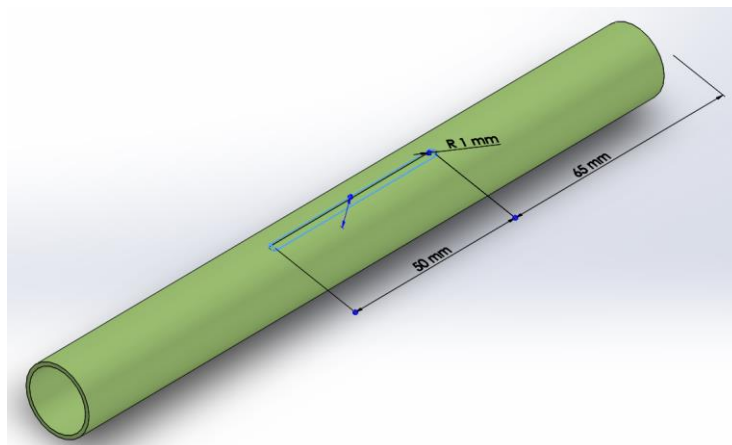


Fig.2 : Schematic illustration of type 6 specimen with a 0.6 mm slot depth and displayed slot dimensions. Each specimen is 180 mm long and has 16 and 18 mm inner and outer diameter.

Table 1. Specimen types according to slot lengths and slot distance to specimen tips

Specimen Type Number	1	2	3	4	5	6	7	8	9	10	11	12	13	14	15	16	17	18	19	
Slot length (mm)	0	10	20	30	40	50	60	70	80	90	100	110	120	130	140	150	160	170	180	
Slot distance from the tip (mm)	-	85	80	75	70	65	60	55	50	45	40	35	30	25	20	15	10	5	0	
Slot tip radius (mm)	-	1	1	1	1	1	1	1	1	1	1	1	1	1	1	1	1	1	1	-

The finite element models were developed and analyzed according to the given material and geometrical specifications. Glass-fiber and epoxy matrix elastic properties and endurance limits used in the numerical solution can be found in Table 2. Quasi-static torsional

loads were applied on to the free ends of the composite tube specimens where other ends are fixed.

Table 2. Orthotropic properties of E-glass fiber reinforced epoxy based composite material

Density $\times 10^{-9}$ kg/m ³	Young's Modulus in dir. x (MPa)	Young's Modulus in dir. y (MPa)	Young's Modulus in dir. z (MPa)	Poisson's Ratio xy	Poisson's Ratio yz	Poisson's Ratio xz	Shear Modulus xy (MPa)	Shear Modulus yz (MPa)	Shear Modulus xz (MPa)
1.85	35000	9000	9000	0.28	0.4	0.28	4700	3500	4700

3. RESULTS AND DISCUSSION

The glass fiber reinforced epoxy tubes with 16 mm inner and 18 mm outer diameter and with a total length of 180 mm was subjected to a 10 Nm static torsional load from one end while the other end is fixed. Finite element models (FEM) were developed to define two types of composite tube structures as $[(0/90)_5]$ and $[(\pm 45^\circ)_5]$ fiber orientations.

The tubes were deliberately defected by longitudinally extending, 0.6 mm deep and 2 mm wide but varying-length slots. An appearance of a meshed geometry relating to the 50 mm long slot with locally refined element sizes is given Fig. 3. The both ends of the slot clearance were rounded at a radius of 1 mm, which is formed by the shape of the milling cutter.

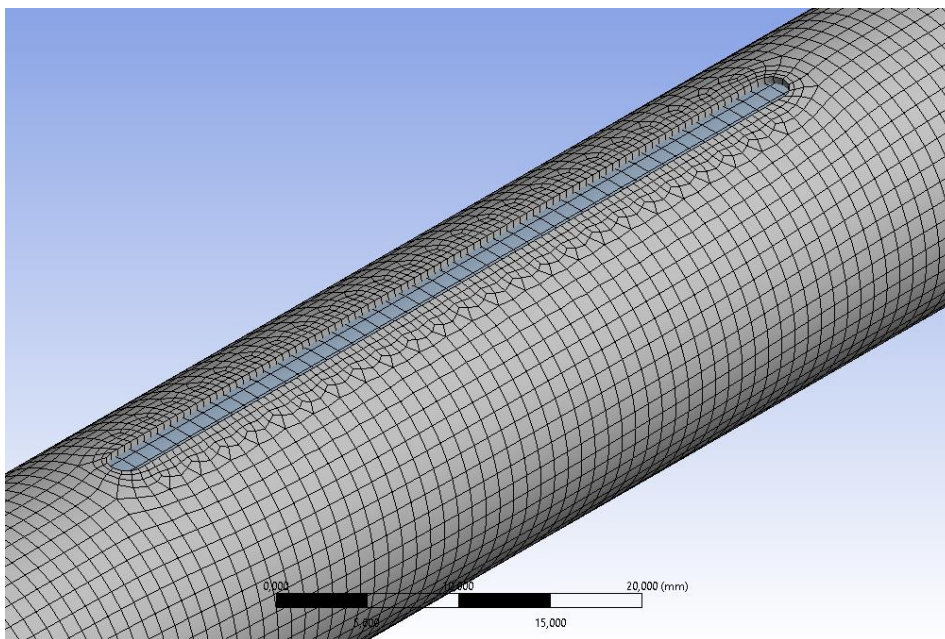
**Fig.3 :** Mesh configuration in the vicinity of the slot for the type 6 specimen

Fig. 4 illustrates equivalent Von-Mises stress distribution on the outermost laminate of the type 6 (see Table 2) epoxy based specimen with $[(0/90)_5]$ glass fibers during the application of a static load of 10 Nm Torsional Moment. Apparently, maximum stress was measured as around 60 MPa in red colored areas of the outermost layer of the tube structure. Although the most critical region and the highest stress concentration is found to appear on both sides of the slot line near the tip of the tube, it is clear that at least a part of the slot perimeter is also affected by the stress accumulation with about 45 MPa stress level according to the color chart. Thus, the notch effect based on the discontinuity formed by the slot cavity at the outermost layer must also not be ignored. Conversely, remaining parts of the slot vicinity exhibited the lowest stress values with a

substantial stress relaxation.

Generally, in comparison to those of measured in the outermost lamina, the stresses in innermost lamina have been found as far more severe according to Fig. 5, and reaches to 74.022 MPa at some points. The maximum stress marker and red areas are located at the extreme end of the tube; however these high stresses are doubtlessly originated by the stress accumulation due to limited load application area. This type of intensifications can be easily eliminated by expanding the load application surface. As for the other regions, the actual stress intensity occurs in the area below the tip of the slot clearance at nearly 60 MPa, which is about 33.3 % higher than that calculated in the slot vicinity but nearly the same as calculated in the most critical region of the outermost layer.

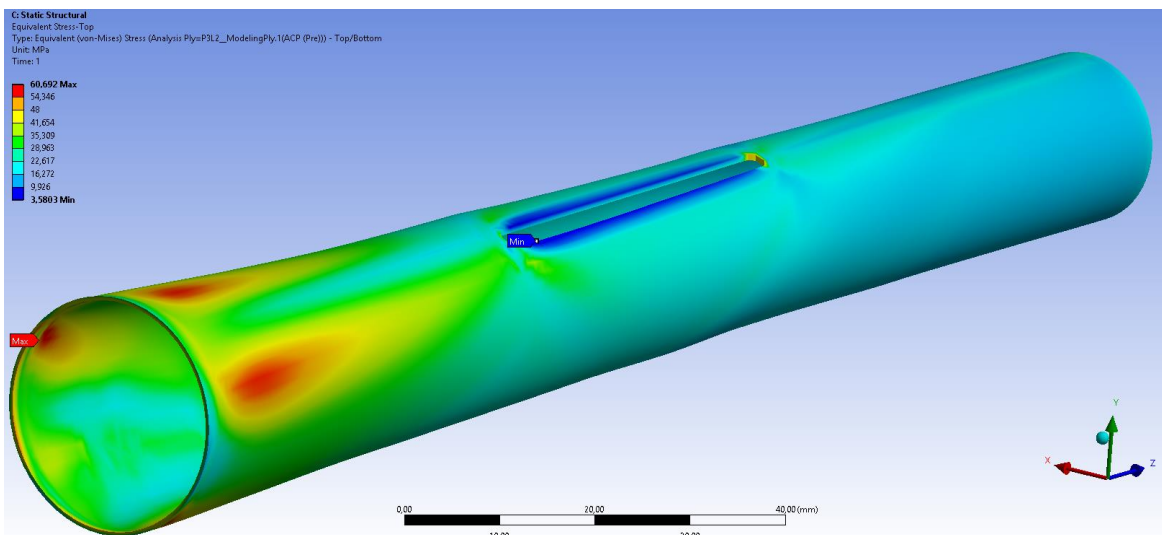


Fig.4 : Equivalent Von-Mises stress distribution on the outermost lamina of the type 6 specimen with $[0/90/0/90/0/90/0/90/0/90]$ fiber orientations

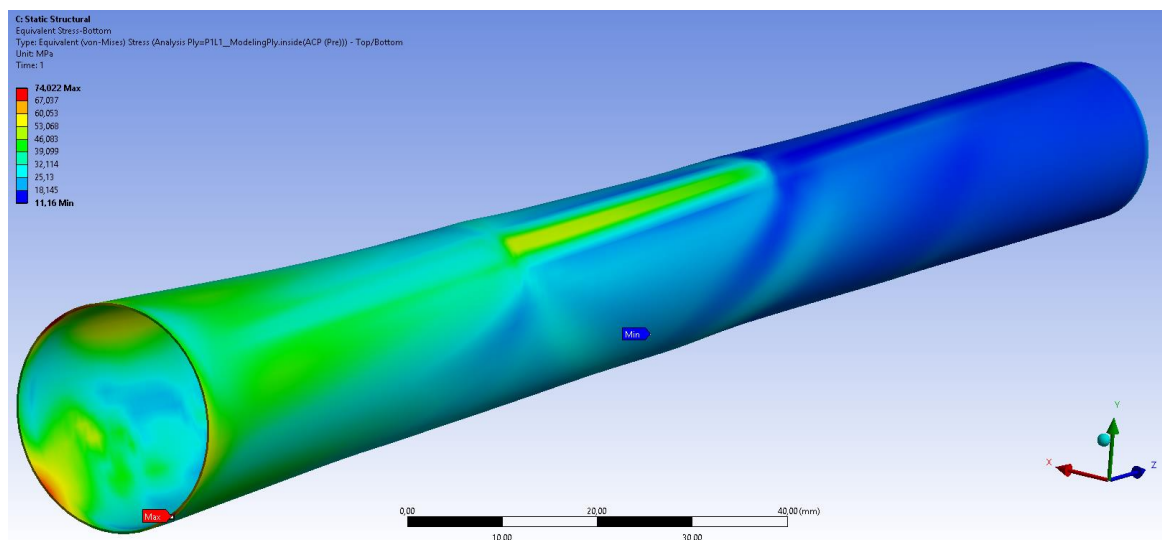


Fig.5 : Equivalent Von-Mises stress distribution on the innermost layer of the type 6 specimen with $[0/90/0/90/0/90/0/90/0/90]$ fiber orientations

Unlike the $[(0/90)_5]$ oriented specimen type, the maximum stress intensification at the outermost lamina is seen at a tip of the slot perimeter of the tube with a $[(\pm 45^\circ)_5]$ laminated structure (Fig. 6). The remaining stress accumulations are about the same as observed in $[(0/90)_5]$ oriented structure in terms of value as well as location. As for the innermost lamina which has not been damaged by milling process, stress concentration below the slot clearance reaches to a level of almost 70 MPa, whereas maximum stress is found to be as 85.554 MPa exactly in the load application region. Thus, comparing with $[(0/90)_5]$ laminate, it can be said for $[(\pm 45^\circ)_5]$ fiber oriented structure that, relatively higher stresses are generated by the same torsional load, not only

in the circumferential and subjacent areas of slots, but also in the load application zone of the tube specimen. Stress accumulation regions observed at the innermost lamina of $[(\pm 45^\circ)_5]$ filament wound specimen (Fig. 7) seem to be analogous with the $[(0/90)_5]$ pre-preg tube specimen except for the stress values. Approximately, 18.75 % increase in equivalent stress level is measured under slot clearance area when $[(\pm 45^\circ)_5]$ filament wound material is used instead of $[(0/90)_5]$ laminated structure. Besides this, the maximum stress value detectable at any point also increased by 15.58 % at the extreme end of the innermost layer of the $[(\pm 45^\circ)_5]$ structure in comparison to that of the $[(0/90)_5]$ structure.

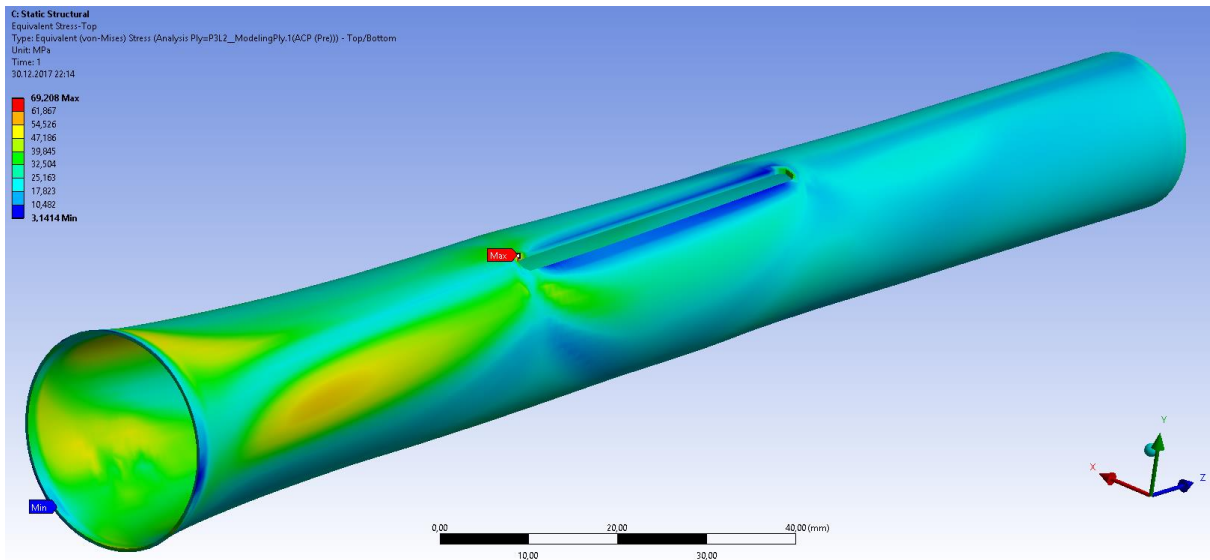


Fig.6 : Equivalent Von-Mises stress distribution on the outermost layer of the type 6 specimen with $[45/-45/45/-45/45/-45/45/-45/45/-45]$ fiber orientations

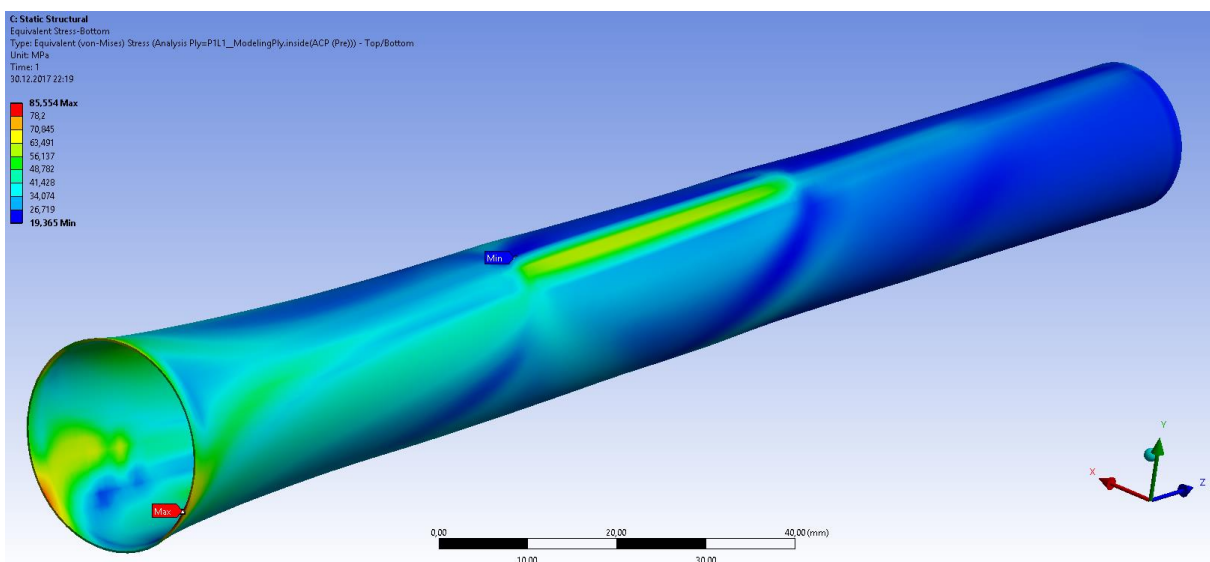


Fig.7 : Equivalent Von-Mises stress distribution on the innermost layer of the type 6 specimen with $[45/-45/45/-45/45/-45/45/-45/45/-45]$ fiber orientations

Maximum stresses are observed to be also changeable according to slot lengths in axial direction and the variation can be said to be not in a linear manner in outermost layer according to Fig. 8. This unsteadiness in stress increase in case of slot length change is probably caused from the fiber discontinuities in outermost layer which inhold the slot cavity. Considering that slot lengths of 0 and 180 mm represent tubes with slot-less and full length slots, respectively, the changes in maximum stresses of the outermost layer displays a fluctuating course. The slotless geometry of the laminated materials made of both $[(\pm 45^\circ)_5]$ and $[(0/90)_5]$ stacking sequences, give the same top stress levels, however different state of stresses takes place on outermost lamina of each specific model in the case of the presence of the slot cavity. It is worth noting that the maximum stress measured as 83.195 MPa at outermost layer of $[(0/90)_5]$ laminate develops when slot length is 30 mm, whereas the $[(\pm 45^\circ)_5]$ laminated specimen with 170

mm slot length gives the maximum outermost lamina stress as 83.399 MPa. In other words, the maximum stress levels reaches at an analogous peak point at different slot lengths in both types of structure with dissimilar fiber orientations.

Another striking point is that the calculated maximum stress at the outermost layer of the slot-less $[(\pm 45^\circ)_5]$ structure is the same as that of the thoroughly slotted $[(\pm 45^\circ)_5]$ structure. This suggests that discontinuous longitudinal cuts in tubular structures made of $[(\pm 45^\circ)_5]$ fibers are more damaging as compared to continuous shallow cuts. However, it is not right to use the same expression for $[(0/90)_5]$ prepreg composite tube constructions. Because, when the maximum stress points in this structure are examined, it is obvious that there is a clear difference of 16,193 MPa between the slot-less structure and the thoroughly slotted $[(0/90)_5]$ structure.

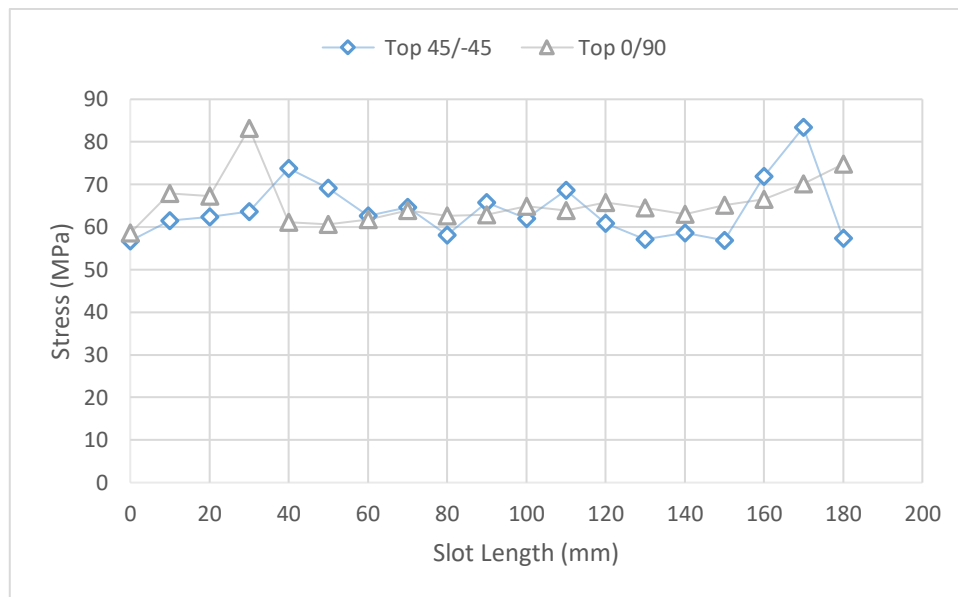


Fig.8 : Maximum von-mises stress level detected on the outermost layer of the filament wound tubes of different slot lengths

As regards the maximum stress variation in the innermost layer (Fig. 9), a regular increase in the maximum stress can be detected as the case changes from slot-less to full-length slotted tube structure (0-180 mm), contrary to the situation on the outermost layer. None the less, the slot-less structures of two different material types ($[(\pm 45^\circ)_5]$ and $[(0/90)_5]$) of stacking sequence give very close values, just as the situation observed in the outermost layer. When switched to the slotted structure, two sort of material model display a marked difference in maximum stresses and the difference gets even larger starting from 140 mm slot length to full

length slot. While the top maximum stress between two sorts of material in the outermost layer varies according to the slot lengths as seen in Fig. 8, the innermost layer with the highest maximum stress is continuously the 45° angle lamina, regardless of slot length. In general, it can be acknowledged for both of the material models that, the stress state at the innermost layer changes with respect to the slot length more smoothly than that measured at the outermost layer. The situation proves that the stress state at the innermost lamina which has not been affected by slot damage is more predictable for any length of void defect.

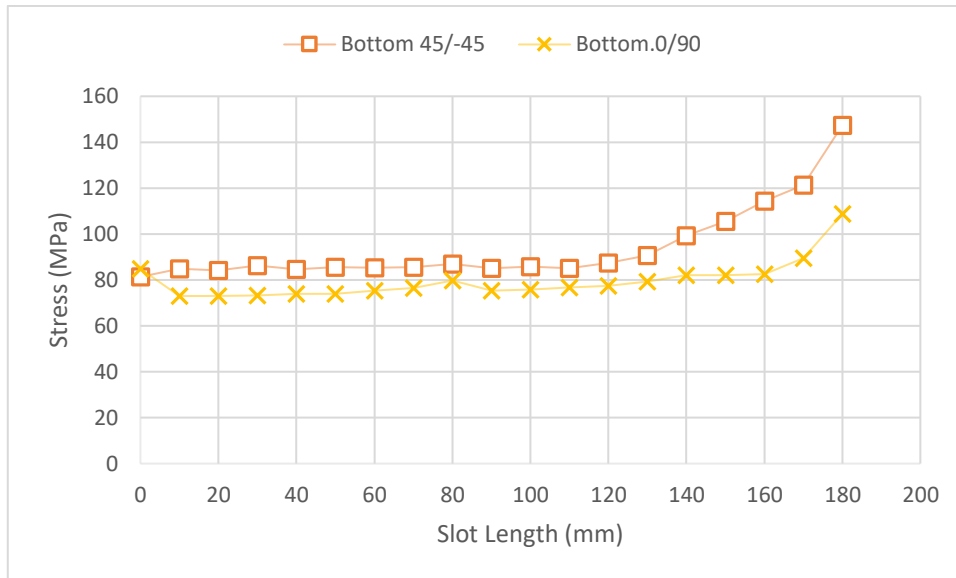


Fig.9 : Maximum von-mises stress level detected on the innermost layer of the filament wound tubes of different slot lengths

Maximum strains detected at outermost and innermost lamina are presented in Fig. 10 and Fig. 11, respectively. As a result of 10 Nm torsional moment, the structure with 45°/-45° oriented fibers has apparently highest maximum strains at the outermost lamina between 30 mm and 120 mm slot lengths, whereas the 0°/90° structure exhibited further amount of deformation under and above the specified range. In both of the structures, it is possible to define three characteristic maximum elastic strain regions separated by 30 and 120 mm vertical lines. Interestingly, values in both structures exhibit an opposite state of maximum stress to each other. This can be attributed that the principal and maximum shear stress axes in pure torsion coincide with the

winding directions in both structures. On the other hand, maximum strain levels detected at the innermost lamina of the both structures have also three characteristic regions separated by 20 and 160 mm vertical lines. In the maximum strain levels of the both structures, a rapid increase in the first part of slot lengths (0-20 mm), fluctuations in opposite directions in the second part (20-160 mm), and a more sudden increase in the last part (160-180 mm) are visually detected. The situation gives a clue about which distance from the slot tip to the tube end is starting to be critical in torsion for fiber reinforced plastic tubes made of angle and cross-ply laminates.

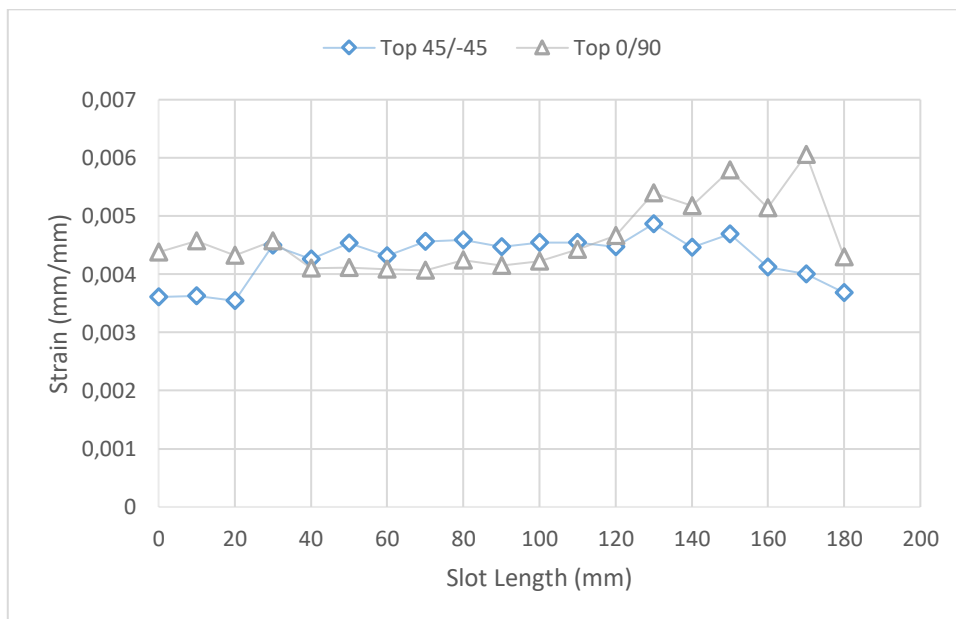


Fig.10 : Maximum strain levels detected on the outermost layer of the filament wound tubes of different slot lengths

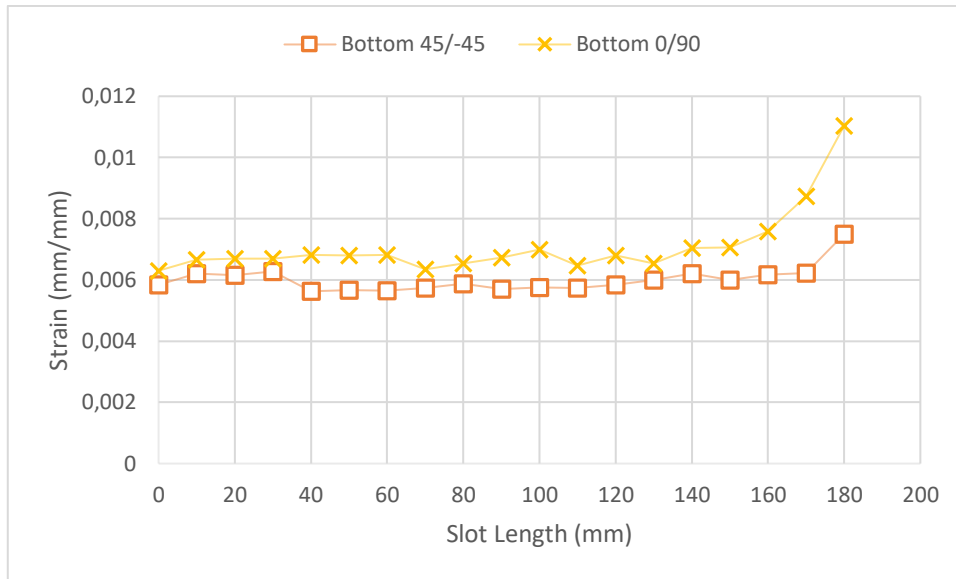


Fig.11 : Maximum strain levels detected on the innermost layer of the filament wound tubes of different slot lengths



Fig.12 : Maximum twisting angles detected on the tip of the of the 18 mm long filament wound tubes of different slot lengths

The total rotation angles at the extreme ends of the tubes shown in Fig. 12 are one of the most prominent results of the current study. The first notable point here is that there is a significant difference in rotation angle between the two tube structures that differ in terms of fiber orientation. The difference in twist angle between two structures begins with the slot-less tube and is maintained up to the vertical border representing the full slot specimen. Although it varies for each slot length, there is an average difference of 0.66° between the rotation angles of two separate types of structures for all slot lengths. Another important aspect related with the curves is that the slots longitudinally

processed on the outer surfaces of the hollow cylindrical specimens significantly increase the twisting angle in both cases of $[(\pm 45^\circ)_5]$ and $[(0/90)_5]$ structures despite a slight geometric defect created deliberately. When the situation of the $45^\circ/-45^\circ$ angle-ply structure is examined, the twist angle measured as 2.72° in the slot-less case increased by 8.32 % up to the case of full-length slot, in association with extended slot length. It is also possible to observe a similar increase when $0^\circ/90^\circ$ structure is investigated. While the amount of angular deformation at the end of the flawless structure is limited to 3.36° , it reached up to 3.67° during the examination of full-length slotted structure, by an

increase of 9.11 %. This can be regarded as an indication of the importance of longitudinal slots in thin-walled cylindrical composite structures and how much the torsion resistance tends to decrease depending on the slot length.

4. CONCLUSION:

Torsional loading responses of two types ($[(\pm 45^\circ)_5]$ and $[(0/90)_5]$) of hollow thin-walled (1 mm) cylindrical tubes (with 16 mm inner diameter and 180 mm length) were investigated throughout the current numerical examination. The effects of rounded end, 2 mm wide and 0,6 mm deep slots created in longitudinal direction were investigated under 10 Nm constant torsional loading condition for the two specified kind of structure. Based upon the results of the study the following conclusions can be made:

- While the notch effect based on the discontinuity formed by the slot cavity at the outermost layer is non-negligible at the slot tip, remaining parts of the slot vicinity exhibits a substantial stress relaxation. It may be advisable to reinforce the specified end piece to prevent the risk of progression of the slot-like damage.
- Although stress accumulation regions observed under slot clearance at the innermost lamina are very similar to each other, $[(\pm 45^\circ)_5]$ filament wound specimen exhibits 18.75 % higher equivalent stress value than $[(0/90)_5]$ laminated structure under the same torsional moment which allows developing of a greater load capacity.
- Maximum stresses are observed to increase as the slot lengths extended in axial direction and the variation can be said to be not in a linear manner in outermost layer which probably caused from the fiber discontinuities.
- Contrary to the situation on the outermost layer, a regular increase in the maximum stress can be detected in the innermost layer as the case changes from slot-less to full-length slotted tube structure (0-180 mm).
- Both in innermost and outermost layer, the slot-less structures of two different material types ($[(\pm 45^\circ)_5]$ and $[(0/90)_5]$) generate very close maximum stresses. However, two sort of material model display a marked difference in maximum stresses especially for slot lengths longer than 140 mm.
- The total twisting angles at the extreme ends of the tubes with $[(0/90)_5]$ stacking sequence are 0.66° greater than those with $[(\pm 45^\circ)_5]$, on average.
- The twisting angles increase in both structures as the slot lengths are extended. This increase is detected as 8.32 and 9.11 % in the $45^\circ/-45^\circ$ angle-ply and $0^\circ/90^\circ$ cross-ply structures, respectively.

REFERENCES

- [1] G. Meijer, F. Ellyin, "A failure envelope for $\pm 60^\circ$ filament wound glass fibre reinforced epoxy tubulars", *Composites: Part A*, vol. 39, pp. 555–564, 2008.
- [2] I. Burda, A.J. Brunner, M. Barbezat, "Mode I fracture testing of pultruded glass fiber reinforced epoxy rods: Test development and influence of precracking method and manufacturing", *Engineering Fracture Mechanics*, vol. 149, pp. 287-297, 2015.
- [3] G. Perillo, R. Vacher, F. Grytten, S. Sørbo, V. Delhayé, "Material characterisation and failure envelope evaluation of filament wound GFRP and CFRP composite tubes", *Polymer Testing*, vol. 40, pp. 54-62, 2014.
- [4] LAL. Martins, FL. Bastian, TA. Netto, "Structural and functional failure pressure of filament wound composite tubes", *Materials and Design*, vol. 36, pp. 779–787, 2012.
- [5] LAL. Martins, FL. Bastian, TA. Netto, "Reviewing some design issues for filament wound composite tubes", *Materials and Design*, vol. 55, pp. 242–249, 2014.
- [6] EV. Morozov, "The effect of filament-winding mosaic patterns on the strength of thin-walled composite shells", *Composite Structures*, vol. 76, pp. 123–129, 2006.
- [7] F. Hafeez, F. Almaskari, "Experimental investigation of the scaling laws in laterally indented filament wound tubes supported with V shaped cradles", *Composite Structures*, vol. 126, pp. 265–284, 2015.
- [8] J. Xing, P. Geng, T. Yang, "Stress and deformation of multiple winding angle hybrid filament-wound thick cylinder under axial loading and internal and external pressure", *Composite Structures*, vol. 13, pp. 868–877, 2015.
- [9] P. Mertiny, F. Ellyin, A. Hothan, "An experimental investigation on the effect of multi-angle filament winding on the strength of tubular composite structures", *Composites Science and Technology*, vol. 64, pp. 1–9, 2004.
- [10] P. Krishnan, MS. AbdulMajid, M. Afendi, AG. Gibson, HFA Marzuki, "Effects of winding angle on the behaviour of glass/epoxy pipes under multiaxial cyclic loading", *Materials and Design*, vol. 88, pp. 196–206, 2015.
- [11] HH. Moreno, B. Douchin, F. Collombet, D. Choqueuse, P. Davies, "Influence of winding pattern on the mechanical behavior of filament wound composite cylinders under external pressure", *Composites Science and Technology*, vol. 68, pp. 1015–1024, 2008.
- [12] D. Tele, N. Wakhare, R. Bhosale, P. Bharde and S. Nerkar, "A Review on Design and Development of Filament Winding Machine for Composite Materials", *International Journal of Current Engineering and Technology*, vol.6, pp. 2347 – 516, 2016.
- [13] ASTM D5448/D5448M-11 Standard Test Method for Inplane Shear Properties of Hoop Wound Polymer Matrix Composite Cylinders.
- [14] ASTM D6507-16 Standard Practice for Fiber Reinforcement Orientation Codes for Composite Materials